



# Nitrogen-doped carbon dots as an effective fluorescence enhancing system for the determination of perfluorooctyl sulfonate

Like Lin<sup>1</sup> · Shuigen Zhou<sup>1</sup> · Huiqin Guo<sup>1</sup> · Yanfei Chen<sup>1</sup> · Sen Lin<sup>1</sup> · Liushui Yan<sup>1</sup> · Kexin Li<sup>1</sup> · Jing Li<sup>1</sup>

Received: 15 January 2019 / Accepted: 12 May 2019 / Published online: 27 May 2019  
© Springer-Verlag GmbH Austria, part of Springer Nature 2019

## Abstract

Nitrogen-doped carbon dots (NCDs) were synthesized via hydrothermal treatment of vitamin B1 and triethylamine. The NCDs exhibit strong blue fluorescence (with a peak at 437 nm at an excitation wavelength of 370 nm), good water solubility and excellent fluorescence stability in the pH 3~12 range, at ionic strengths between 0.01 and 1 M, and under UV illumination for 6 h, as well as incubation temperature of 15~60 °C. The nanoparticles respond selectively and sensitively to trace concentrations of perfluorooctane sulfonate (PFOS) through electrostatic interactions between PFOS and NCDs. This is accompanied by the aggregation of NCDs to yield enhanced fluorescence. The nanoprobe has high selectivity for PFOS even in presence of other common ions such as metal ions, anions, and structural analogues such as surfactants. Under the optimal conditions, the response is linear in the 0.3 to 160 nM PFOS concentration range with a detection limit of 0.3 nM. Satisfactory results were achieved for determination of PFOS in spiked real water samples.

**Keywords** Nitrogen-doped carbon dots · PFOS · Fluorescence enhancement · Surface water samples

## Introduction

Perfluorinated compounds (PFCs) were first produced in 1951 by the 3M company. They became increasingly utilized,

particularly in firefighting foams, lubricants, surfactants, and various other industrial and consumer products [1, 2]. Perfluorooctane sulfonate (PFOS) is a perfluorochemical issued from final conversion of many PFCs. It is nondegradable pollutant detected worldwide in surface water, activated sludge, air, soil, animals, plants, and human [3]. Due to the bioaccumulation [4] and toxicity [5] of PFOS, its migration, transformation, and pollution status in the environment has attracted increasing attention by the research community [6]. As one of the emerging chemical pollutants [7], PFOS has been regulated under the Stockholm Convention on persistent organic pollutant in 2009 [8]. The interim health assessment report by the U.S. Environmental Protection Agency (USEPA) and Water Framework Directive (WFD) of European Commission give permit of the PFOS concentration. It is allowed to 200 ng·L<sup>-1</sup> [9] and 0.65 ng·L<sup>-1</sup> [10] in drinking water and fresh water, respectively. It has reported that PFOS concentration in the surface water was 2.89~13.07 ng·L<sup>-1</sup> [11, 12]. Tremendous efforts have recently been devoted to developing appropriate quantitative analysis methods of PFOS for environmental monitoring and assessment, water quality protection, and disease prevention. So far, many analysis techniques are used for PFOS, including liquid chromatography-mass spectrometry (LC-MS) [13], liquid chromatography-mass/mass spectrometry (LC-MS-MS)

---

Like Lin and Shuigen Zhou contributed equally to this work.

## Highlights

- 1) Nitrogen-doped carbon dots are a viable nanoprobe for PFOS detection
- 2) The detection strategy is based on fluorescence enhancement with LOD of 0.3 nM
- 3) The nanoprobe is sensitive and selectivity for PFOS detection in water samples

---

**Electronic supplementary material** The online version of this article (<https://doi.org/10.1007/s00604-019-3501-y>) contains supplementary material, which is available to authorized users.

✉ Huiqin Guo  
guohuiqin@nchu.edu.cn

✉ Liushui Yan  
yanliushui@nchu.edu.cn

<sup>1</sup> Key Laboratory of Jiangxi Province for Persistent Pollutants Control and Resources Recycle, School of Environmental and Chemical Engineering, Nanchang Hangkong University, Nanchang 330063, China

[14], and gas chromatography-mass spectrometry (GC-MS) [15]. However, these methods suffer from some disadvantages, such as complicated operation, time consuming and expensive cost. Fluorescence spectrophotometry has rapidly developed because it is simple, rapid and sensitive properties, which attracts more and more attention.

Carbon dots (CDs) are carbon nanomaterials with sizes smaller than 10 nm [16]. Compared to traditional organic fluorescent dyes, fluorescent CDs have distinguishable characteristics, including high resistance to photo bleaching, wide excitation spectra, robust chemical inertness, low toxicity, and good biocompatibility [17]. Hence, they attracted tremendous attention and have widely been applied in many fields, such as bioimaging [18], drug delivery [19], fluorescent sensors [20], and optoelectronic devices [21]. As fluorescence or electrochemical sensors or probes, they attracted tremendous attention and have widely been applied in determination of persistent organic pollutants or emerging chemical pollutants [22–25]. For PFOS detection, Tan and coauthors [26] prepared fluorescent CDs through one-step hydrothermal route. Then they developed fluorescent visual and turn-on method for detection of PFOS through fluorescent carbon dots and berberine chloride hydrate (BH). They also constructed a triple-channel optical (fluorescence, UV-vis and resonant light scattering) PFOS analytical system, based on the reaction between CDs and PFOS leading to three signals changes [27]. High sensitivity was obtained and the detection limit was lower to about  $20 \text{ nmol}\cdot\text{L}^{-1}$  in these reports. Jiao et al. [28] recently reported a molecularly imprinted chitosan doped with carbon quantum dots, for fluorometric determination of perfluorooctane sulfonate. The detection was based on the fluorescence emission of carbon quantum dots at 460 nm was enhanced in addition of PFOS. A linear range of  $20\text{--}200 \text{ pg}\cdot\text{L}^{-1}$  and detection limit of  $66\text{--}85 \text{ pg}\cdot\text{L}^{-1}$  was obtained. These successful works provide novel strategies for rapid and sensitive detection of PFOS. However, limited studies were reported especially on the mechanism of fluorescence enhancement. It still needs more researches to fabrication of CDs which have excellent luminescence phenomena and more unexpected properties, and explore them as nanoprobes for detection perfluorinated compounds with good selectivity and sensitivity.

In this study, green and high-output hydrothermal strategy was used to prepare highly fluorescent nitrogen doped-carbon dots (NCDs). The fluorescent NCDs were water-soluble and remarkably stable under extreme conditions of pH, temperature and ionic strength. A fluorescent nanoprobes for PFOS was developed based on fluorescence enhancement of NCDs at 437 nm. The probe exhibited high selectivity and sensitivity towards the detection of PFOS in aqueous solution, which was successfully used for trace concentration of PFOS determination in surface water samples.

## Experimental

### Materials

Vitamin B1 (VB1) was purchased from Chengdu Aikeda chemical reagents (Chengdu, China, <http://aikeshiji.net114.com>) and quinine sulfate (QS, BR grade) from Beijing Solarbio Science & Technology (Beijing, China, <http://solarbio.company.weiku.com>). The quantum yield (QY) of the carbon dots was calculated using quinine sulphate (QS). PFOS ( $\geq 95.0\%$  (H-NMR)), perfluorooctanoic acid (PFOA), perfluorohexyl sulfonate potassium (PFHSK), perfluorinated butyl sulfonic acid potassium (PFBSK) and aminoethyl alcohol were all obtained from Sigma-Aldrich China-Mainland (Shanghai, China, <http://www.sigma-aldrich.com>). The molecular structure of PFOS was shown in Fig. 1. Potassium 2-(6-chloro-1,1,2,2,3,3,3,4,4,5,5,6,6-dodecafluorohexyloxy) (F53-B, purity  $\geq 99\%$ ) was purchased from Shanghai Synica (Shanghai, China, <http://synica.company.weiku.com>). Hexadecyltrimethyl ammonium bromide (CTAB), sodium dodecylsulfate (SDS), NaCl, KCl,  $\text{Ca}(\text{NO}_3)_2$ ,  $\text{MgCl}_2$ ,  $\text{CuSO}_4$ ,  $\text{CoSO}_4$ ,  $\text{NiCl}_2$ ,  $\text{FeCl}_3$ ,  $\text{FeCl}_2$ ,  $\text{MnSO}_4$ ,  $\text{BaCl}_2$ ,  $\text{CdSO}_4$ ,  $\text{ZnCl}_2$ ,  $\text{Pb}(\text{NO}_3)_2$ ,  $\text{AgNO}_3$ ,  $\text{Cr}(\text{NO}_3)_3$ ,  $\text{Al}(\text{NO}_3)_3$ ,  $\text{NH}_4\text{Cl}$ ,  $\text{NaHCO}_3$ , ethylenediamine and triethylamine were all received from Xilong Chemical Co., Ltd. (Guangzhou, China, <http://xilongchemical.en.made-in-china.com>). The reagents were all of analytical grade and used as received without further purification. Deionized water prepared with Mili-Q Direct-Q@5UV water purification system (Millipore, Bedford, MA, USA, <http://www.merckmillipore.com>) was used throughout the experiments.

### Preparation of fluorescent nitrogen-doped carbon dots (NCDs)

In a typical synthesis, 1.25 g VB1 was dissolved in 30 mL deionized water under sonication. Next, 1.0 mL triethylamine was then slowly dropped into the solution. The mixture was transferred into a 50 mL teflon-lined stainless steel autoclave and heated at  $200 \text{ }^\circ\text{C}$  for 6 h at heating rate of  $5 \text{ }^\circ\text{C}\cdot\text{min}^{-1}$ . The resultant brown mixture was centrifuged at 4500 g for 10 min to remove the solid and large dots. Afterwards, the resulting solution was concentrated in  $60 \text{ }^\circ\text{C}$  water bath to 2–3 mL and then freeze-dried to obtain NCDs solid. In control experiment, 1.25 g VB1 was placed in an autoclave and heated to  $200 \text{ }^\circ\text{C}$  for 6 h in drying oven to yield CDs. The other procedures were

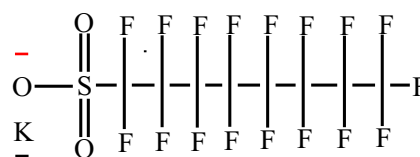


Fig. 1 Molecular structure of PFOS

the same as those employed for NCDs. The obtained nanomaterials were then stored at 4 °C for further use.

## Characterization

The photoluminescence (PL) spectra of NCDs were recorded on a fluorescence spectrometer (F-7000, Hitachi, Tokyo, Japan, <http://www.hitachi.com>), with slit width of 5 nm for both excitation and emission. The UV-Vis absorbance spectra were recorded on a UV-3010 spectrophotometer (Hitachi, Tokyo, Japan, <http://www.hitachi.com>). Fourier transform infrared spectrometry (FT-IR) was conducted on a Nicolet-iS5 spectrometry (Massachusetts, U.S., <http://www.thermofisher.com>) using KBr pellets. Transmission electron microscopy (TEM) with X-ray energy dispersive spectroscopy (EDS), and high-resolution transmission electron microscopy (HRTEM) were conducted on a FEI TalosF200X field emission (Massachusetts, U.S., <http://www.thermofisher.com>). X-ray photoelectron spectroscopy (XPS) was performed on an Axis Ultra DLD instrument (Shimadzu, Japan, <https://www.shimadzu.com>) with monochromated Al-K $\alpha$  source at residual gas pressure below  $10^{-8}$  Pa. X-ray diffractometer (XRD) spectrum were obtained by Rigaku Ultima IV (Tokyo, Japan, <http://www.rigaku.com>). The zeta-potentials of NCDs water suspensions at pH from 3 to 12 (adjusted by diluted NaOH or H $_2$ SO $_4$ ) were determined using zeta potential meter (Zetasizer Nano-ZS90, Malvern, <https://www.malvernpanalytical.com>).

## Detection of PFOS with NCDs

The detection of PFOS was performed in aqueous solution at room temperature. In a typical detection procedure, the stock solution of PFOS ( $c = 1 \times 10^{-3}$  mol·L $^{-1}$ ) was first dissolved in deionized water stepwise. Different concentration of PFOS and certain amount of NCDs was added into 10-mL cuvette, then the solution was diluted into 10 mL using pH = 6.1 BR buffer and mixed thoroughly. The final NCDs concentration and PFOS concentration was 2.5 mg·mL $^{-1}$  and 0, 3, 9, 10, 30, 50, 70, 90, 100, 140, and 160  $\times 10^{-10}$  mol·L $^{-1}$  for a standard plot preparation. After incubated in the room temperature for 10 min, the solutions were transferred into 1-mL quartz cuvettes for fluorescence spectra recording at excitation wavelength of 370 nm. All the experiments were performed in duplicate and the average was obtained. The selectivity and interference measurements procedure were provided in the Electronic Supporting Material (ESM).

## Surface water samples analysis

To evaluate the analytical performances of the developed fluorescent method, river water and lake water were tested. The river water sample were collected from Gan River (Nanchang,

China), and lake water from a lake located at the campus (Nanchang Hangkong University). The surface water samples were first centrifuged at 4500 g to separate solid particles and then filtered off with 0.45  $\mu$ m pore size membrane to remove suspended particles. The samples were heated in oil bath at 105 °C for 30 min then stored at 4 °C for further use. All analyses were finished within 48 h. For a typical determination procedure, 0.1 mL of 25 mg·mL $^{-1}$  of NCDs solution and 1 mL pH = 1.81 BR buffer was added into 10-mL cuvette, and then diluted the mixture volume to 10 mL using the water samples. The final NCDs concentration and pH value was 2.5 mg·mL $^{-1}$  and 6.1 for the system. After incubated in the room temperature for 10 min, the solution was transferred into 1-mL quartz cuvette for fluorescence spectra recording at excitation wavelength of 370 nm. Control experiments were conducted under the same conditions using the deionized water instead of the surface water. The analytical data was obtained by external standard method. The standard addition experiment procedure was provided in the ESM.

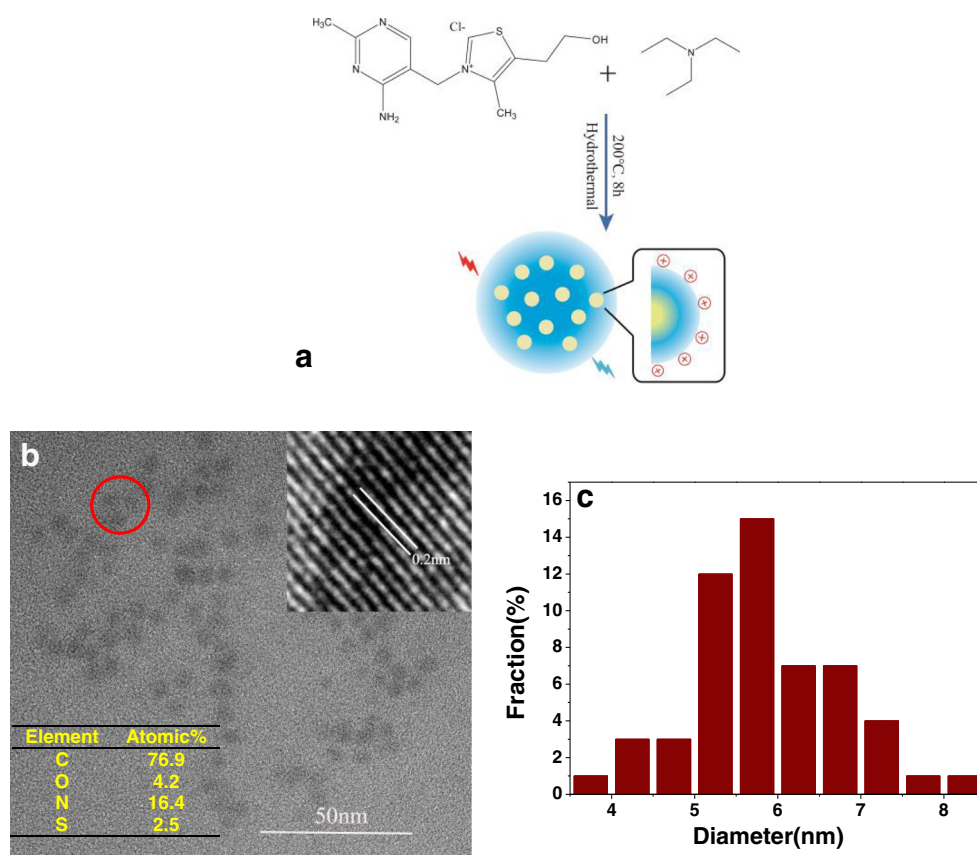
The water samples were also pretreated with solid-phase extraction (SPE) and then analyzed with the fluorescent detection tests, the whole procedure was also provided in the ESM.

## Results and discussion

### Characterization of the nitrogen-doped carbon dots (NCDs)

The synthesis procedure of NCDs was summarized in Fig. 2a. The morphologies and structures of the NCDs are shown in Fig. 2b. The NCDs appeared well monodispersed with uniform sizes. The diameters of NCDs looked relatively narrow in TEM images with main distributions from 5.2–7.2 nm and average size of 5.75 nm (Fig. 2c). The inset in Fig. 2b depicts a representative image of an individual nanoparticle. High crystallinity with lattice parameter of 0.20 nm was observed and corresponding to (102) diffraction plane of graphitic (sp $^2$ ) carbon. However, larger sizes from 6–18 nm with average of 11.25 nm and low stability were noticed for CDs (Fig. S1). The elemental compositions in Fig. 2b (C-76.9%, N-16.4%, O-4.2%, and S-2.5%) and Fig. S1a (C-64.3%, N-8.65%, O-25.3% and S-1.71%) confirmed that percentage of carbon and nitrogen increased in NCDs when compared to CDs, which resulted in the photoluminescence properties greatly improvement. The XRD patterns of the NCDs and VB1 are shown in Fig. S2a. The diffraction peaks of NCDs coincided well with those of the VB1 and were sharper and higher, demonstrating that the prepared NCDs were formed by organic dots, leading to high crystallinity [29], which is consistent with the results of TEM. The XRD pattern of NCDs appeared

**Fig. 2** **a** Illustration on the preparation of NCDs from VB1 and triethylamine, TEM image **b** and corresponding size distribution histograms **c** of synthesized NCDs (the number of particles that has been taken into account to calculate was 94)



a new sharp diffraction peak at  $24.5^\circ$ , which was consistent with the (002) lattice spacing of carbon-based materials [30].

The zeta-potential of NCDs was determined at various pH values and the results are illustrated in Fig. 3a. The NCDs surfaces were always positively charged from pH 3–10, consistent with the FT-IR results in Fig. S2b (ESM), suggesting the presence of numerous amino ion groups. The oxygen-rich and cationic functional groups present on NCDs surfaces improved their hydrophilicities and stabilities in aqueous systems, which would be promising for sensing in aqueous media.

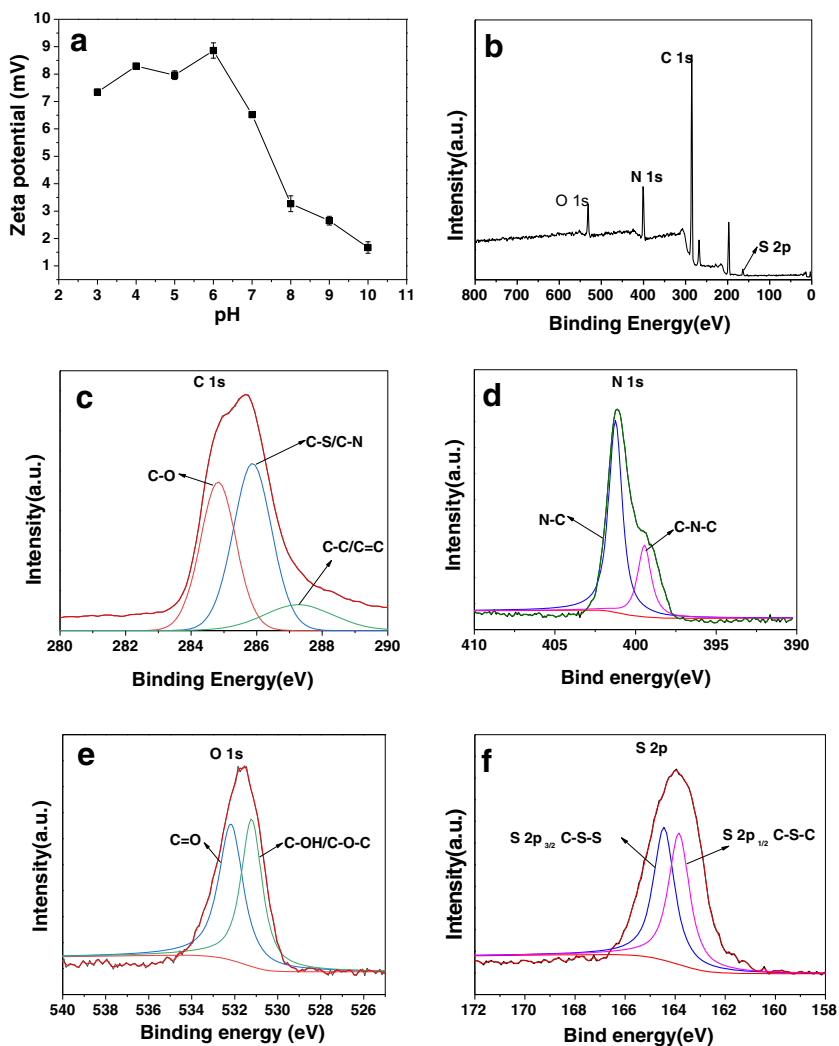
The elemental and functional groups of NCDs were further analyzed by XPS. In Fig. 3b, four peaks at 285, 400, 531.5 and 164.2 eV were observed and attributed to C 1s, N 1s, O 1s and S 2p, respectively. The atomic percentages (at %) of C, N, O and S were recorded as respectively 76.8%, 14.9%, 5.32% and 3.00%, consistent with the EDS results. The detailed peak fitting analyses of C 1s peak of NCDs are gathered in Fig. 3c. The high-resolution C 1s spectra indicated the presence of mainly three different types of carbon bonds: graphitic or aliphatic ( $C=C$  and  $C-C$ ) (284.8 eV), nitrous or sulphurous (285.5 eV), and oxygenated or chlorinated (287.5 eV). The two N 1s peaks present in Fig. 3d testified that nitrogen existed mostly as  $N-(C)_3$ /pyrrolic-N (399.4 eV),  $N-H$ , pyridine-like N or graphitic N (401.3 eV) [31]. Therefore, N was present in  $\pi$ -conjugated systems with two p-electrons, and C atom was replaced by C atom inside NCDs. The enhanced amino N

confirmed the important role of triethylamine in formation of NCDs. The high N content might result in better luminescence properties. The two fitted peaks at 531.2 and 532.2 eV in O1s spectrum (Fig. 3e) were assigned to  $C=O$  and  $C-OH/C-O-C$  groups, respectively. On the other hand, deconvolution of S 1s peak (Fig. 3f) yielded S  $2p_{3/2}$  (163.9 eV) and S  $2p_{1/2}$  (164.4 eV) spin-orbit doublets, attributed to  $C-S-C$  band. Overall, the surface components of NCDs determined by XPS agreed well the FT-IR results.

### Optical properties

Steady-state spectroscopy studies were undertaken to gain a better understanding of the photophysical behaviour of NCDs (Fig. 4). Figure 4a shows the UV-Vis absorption, excitation, and fluorescence spectra of NCDs. The absorption in UV region resulted in generation of two humps at 272 and 320 nm, assigned to the  $n \rightarrow \pi^*$  transition of  $C-O$  and  $C=O$  or  $C-N$  functional groups present at edges of NCDs. The strong absorptions around 232 and 200 nm were ascribed to the  $\pi \rightarrow \pi^*$  transition of conjugated  $C=C$  units in carbon core [32]. Compared with the results of CDs in ESM, it can see that formation of more heteroatomic surface functionalities while using triethylamine doping treatment. The presence of these groups was positively to the fluorescence property of the carbon dots.

**Fig. 3** **a** zeta-potential at different pH values, **b** full range XPS, and high-resolution XPS **c-f** of the NCDs in C1s, N1 s, O 1 s, and S2p binding energy regions



In inset of Fig. 4a, NCDs exhibited bright blue fluorescence under 370 nm irradiation with no obvious absorption peak under 400 nm. With regular increase in excitation wavelength from 330 to 450 nm (Fig. 3b), the fluorescence wavelength

was red-shifted from 423 to 505 nm, showing obvious excitation-dependent behaviour. The maximum excitation and emission wavelengths were estimated to 370 and 438 nm, respectively. The NCDs revealed relatively high

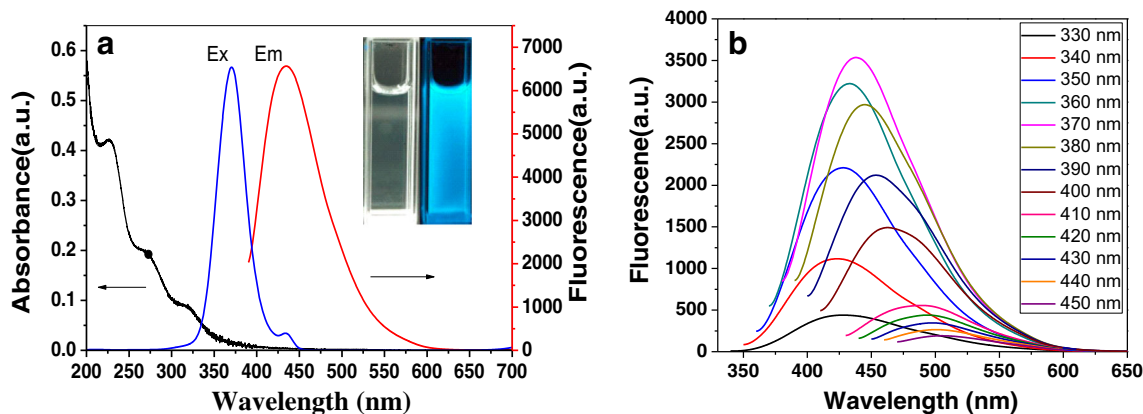
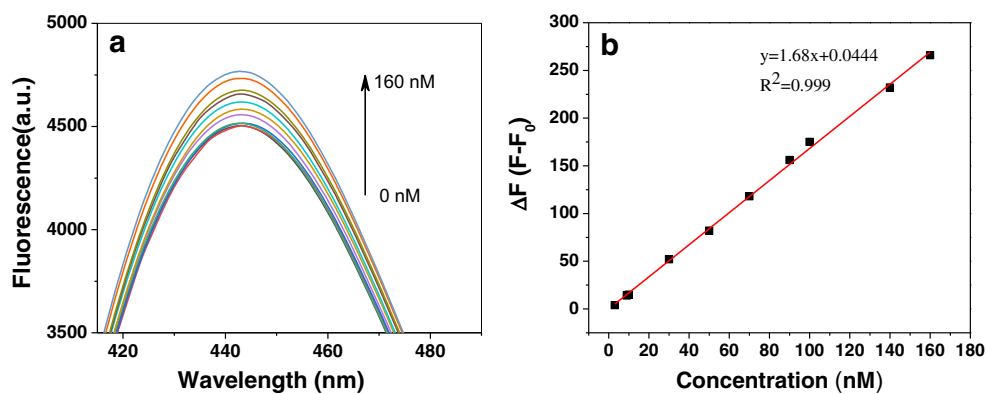


**Fig. 4** **a** UV – Vis absorption (black), excitation (blue), and fluorescence (red) spectra of NCDs. The inset corresponds to NCDs solution at daylight and 370 nm irradiation. **b** Excitation wavelength dependent fluorescence spectra of NCDs

**Fig. 5** **a** Fluorescence enhancement spectra (from bottom to top: 0, 3, 9, 10, 30, 50, 70, 90, 100, 140, and 160  $\times 10^{-10}$  M), **b** The standard plot of PFOS concentration versus  $\Delta F$  (experimental conditions:  $C_{\text{NCDs}} = 2.5 \text{ mg}\cdot\text{mL}^{-1}$ , BR buffer, pH = 6.1, room temperature, excitation wavelength = 370 nm, emission wavelength = 445 nm)



fluorescence quantum yield (QY) of 12%, sufficient for high sensitive photosensors [33] when compared to the smaller QY obtained with CDs (~6%).

### Fluorescence response of nitrogen-doped carbon dots towards PFOS

The stability of NCDs in the impacts of pH, ionic strength and UV radiation time were all examined. The results in ESM showed the highly stable NCDs even under extreme conditions (Fig. S4). Hence, the NCDs were tested for detection of PFOS and determination of the optimal detection conditions, along with the effects of pH, NCDs concentration, and incubation temperature on fluorescence increment was all studied (results shown in Fig. S5). Note that  $\Delta F$  was defined as:  $F - F_0$ , where  $F$  and  $F_0$  represent the fluorescence intensities of NCDs solutions in presence and absence of PFOS, respectively. As shown in Fig. S5a, the value of  $\Delta F$  was high and constant in acidic conditions but started to decrease at pH above 7. This agreed well with zeta-potential result (Fig. 3a), suggesting the important role of the electrostatic interactions between the PFOS and NCDs in PFOS analysis. In Fig. S5b, lower concentration of NCDs solution has high dispersity and positively influenced the analysis. Incubation temperature experiment results in Fig. S5c showed that  $\Delta F$  kept stable in the 15–35 °C, and started to decrease with further temperature increase. Hence, subsequent experiments were performed at pH = 6.1, NCDs concentration of  $2.5 \text{ mg}\cdot\text{mL}^{-1}$  and room temperature.

Figure 5a, b depicts the enhancement in fluorescence emitted by NCDs upon the addition of PFOS. The fluorescence

spectra in Fig. 5a were obtained at different added PFOS concentrations into NCDs solution at excitation of 370 nm. The addition of PFOS from  $3 \times 10^{-10}$  to  $1.6 \times 10^{-8} \text{ mol}\cdot\text{L}^{-1}$  induced gradual increase in fluorescence intensity at 445 nm. The fluorescence increment  $\Delta F$  displayed good linear relationship with PFOS concentration from 3 to  $160 \times 10^{-10} \text{ mol}\cdot\text{L}^{-1}$  (Fig. 5b). The latter suggested an excellent detection threshold of less than 0.3 nM. The method presents a linear range at lower concentration levels and a low LOD, which is comparable to those reported in the literature that using carbon dots or other green probe such as bovine serum albumin [34] for PFOS detection (Table S1). Also, the value for PFOS was a little lower than that allowed by the U.S. Environmental Protection Agency in drinking water (~0.37 nM).

### Selectivity

The complexity of real water composition is challenging to carbon dots during PFOS detection not only in terms of sensitivity but more importantly selectivity. Therefore, selectivity tests were carried to evaluate the performance of the proposed nanoprobe and the results are gathered in Fig. S6. No significant changes in fluorescence were observed for representative ions in water including  $\text{Na}^+$ ,  $\text{K}^+$ ,  $\text{Ca}^{2+}$ ,  $\text{Mg}^{2+}$ ,  $\text{Cu}^{2+}$ ,  $\text{Co}^{2+}$ ,  $\text{Ni}^{2+}$ ,  $\text{Fe}^{3+}$ ,  $\text{Fe}^{2+}$ ,  $\text{Mn}^{2+}$ ,  $\text{Ba}^{2+}$ ,  $\text{Cd}^{2+}$ ,  $\text{Zn}^{2+}$ ,  $\text{Pb}^{2+}$ ,  $\text{Ag}^+$ ,  $\text{Cr}^{3+}$ ,  $\text{Al}^{3+}$ ,  $\text{NH}_4^+$ ,  $\text{SO}_4^{2-}$ ,  $\text{HCO}_3^-$ ,  $\text{Cl}^-$ ,  $\text{NO}_3^-$ , CTAB, SDS, and structural analogues of PFOS (PFBSK, PFHSK and PFOA). However, it showed that F-53B has a little enhancement affect to the fluorescence of NCDs, which is ~16.7% compared to that of PFOS. It suggested that the presence of f-53B may lead

**Table 1** Spiked and recovery tests of PFOS in surface water samples ( $n = 5$ )

Sample	Added ( $\times 10^{-10}$ mol/L)	Found ( $\times 10^{-10}$ mol/L)	Recovery (%)	RSD (%)
River water	10	$10.4 \pm 0.58$	94.9–110	5.64
	30	$28.3 \pm 1.61$	89.3–103	3.64
	50	$50.4 \pm 0.57$	99.6–100	1.13
Lake water	10	$10.1 \pm 0.47$	95.4–107	4.60
	30	$29.1 \pm 0.50$	95.2–99.6	1.70
	50	$49.7 \pm 0.54$	98.7–101	1.09

**Table 2** Determination of PFOS in surface water samples after SPE treatment ( $n = 3$ )

SPE-treated sample	Fluorescent results (nM)	Average (nM)	LC-MS results (nM)	Relative error (%)
Lake water	4.09/4.27/4.30	$4.22 \pm 0.23$	$4.80 \pm 0.37$	-12.1
River water	0.145/0.154/0.150	$0.15 \pm 0.009$	$0.135 \pm 0.012$	+11.2

to false positive results in the determination of PFOS, making the results more inclined to be the total amount of such compounds.

To test the coexistence of interference ions for PFOS detection with the nanoprobe, the fluorescence competition experiments were also performed. In the test, PFOS were added to NCDs after addition of environmentally relevant concentrations of above ions. It will be noted that fluorescence increment of NCDs was changed about +20% in presence of competing ions mixtures. However, fluorescence increment for PFOS in presence of competing ions mixtures was well consistent with the control group (NCDs solution+BR buffer+PFOS). This high specificity is attributed to strong interactions between the active sites of NCDs and low concentration PFOS when compared to other ions. In sum, the NCDs looked suitable for PFOS detection.

### Determination of PFOS in real water samples

Since the fluorescence of NCDs efficiently enhanced in presence of PFOS, the proposed nanoprobe was applied to PFOS detection in real water samples. Pretreated river and lake waters were first spiked with working solutions containing different PFOS concentrations (1, 3, and 5 nM) and then tested using the nanoprobe. The recoveries of PFOS in water

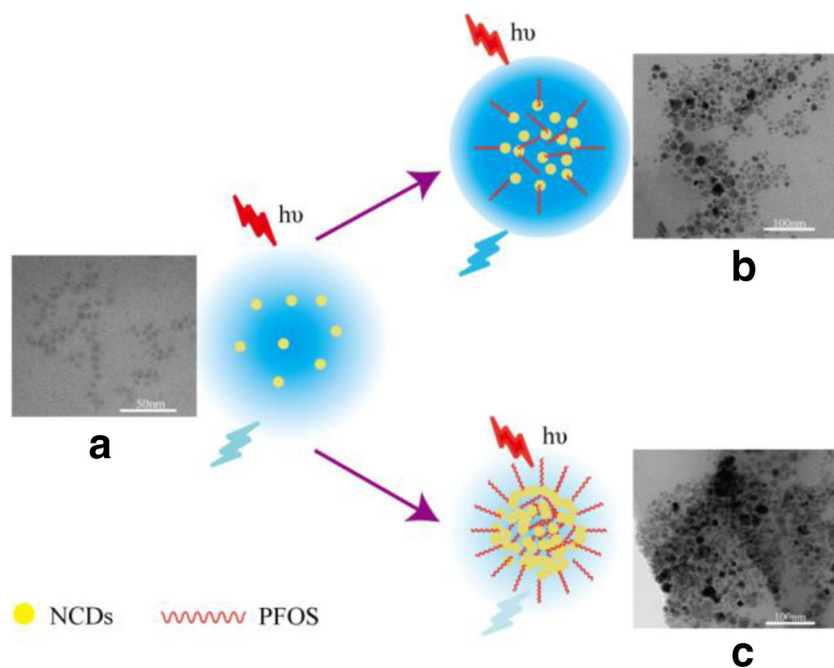
samples were statistically close to 100% and fluctuated from 89.3% to 110% (Table 1). The determination results of PFOS after SPE treatment are listed in Table 2. The fluorescent analyses agreed well with LC-MS analyses with relative errors ranging from -12.1% to +11.2%.

It should be noted that from the results of Table 1, the PFOS concentration in the lake water sample was determined to be 4.22 nM, which locates in the range of the linear range of the fluorimetric method. It is probably that the trace PFOS existed in the water was deeply combined with the matrix, resulting in no PFOS was detected with the direct nanoprobe analysis operation. However, in the spike experiments, the freshly added PFOS may not interact with the matrix, resulted in that PFOS that lowers to 1~5 nM can be detected with high recovery rate and low RSD. Hence, for low PFOS concentration in the environmental water samples, the SPE-treatment or other proper treatment procedure was recommended for a satisfactory determination results.

### Possible enhancement mechanism for PFOS analysis

According to the characterization data, there are abundant functional groups such as -COOH, -OH, N-H, pyrrolic-N, or pyridine-like N in NCDs surface. The amino-groups have been reported to increase the surface passivation of carbon

**Fig. 6** Schematic illustration of fluorescence enhancement detection of PFOS by NCDs. TEM images of NCDs at different concentration of PFOS: (a) 0, (b)  $1 \times 10^{-8} \text{ mol}\cdot\text{L}^{-1}$ , and (c)  $1 \times 10^{-6} \text{ mol}\cdot\text{L}^{-1}$



dots. The pyridinic and pyrrolic nitrogen atoms can be regarded as defect structures because they break the large conjugated carbon structure. The formation of these defects would lead to formation of more polyaromatic structures and give rise to stronger emission [35], which was also evidenced by the FT-IR (Fig. S2b-c) and fluorescence QY results. The surface of NCDs was positively charged in the experiment conditions. When trace PFOS was added into the NCDs solution, it can combine with the amino groups of the nanoprobe through electrostatic interaction or PFOS-NCDs complex, enhancing the conjugation degree of H<sub>2</sub>N-passivated NCDs. This will result in the fluorescence emission enhancement. Similar results were demonstrated in Jiao et al.' report [28]. However, high concentration of PFOS may aggregate to semi-micelle and coat in the surface of the NCDs. This can result in the strongly aggregation of the NCDs, and negatively affected the photoluminescence property of NCDs. To gain a better understanding of the detection reason, the sensing mechanisms were investigated and schematically displayed in Fig. 6. Trace concentration of PFOS ( $1 \times 10^{-8} \text{ mol}\cdot\text{L}^{-1}$ ) combined with NCDs resulted in a moderate aggregation of the nanoprobe, and accompanied by emission enhancement at 445 nm (Fig. 6b). However, high PFOS concentrations ( $1 \times 10^{-6} \text{ mol}\cdot\text{L}^{-1}$ ) would induce strong aggregation of NCDs and yield fluorescence quenching to some extent (Fig. 6c and Fig. S7). As PFOS concentrations were above to  $1.6 \times 10^{-8} \text{ mol}\cdot\text{L}^{-1}$  (Fig. S7),  $\Delta F$  significantly reduced until reaching negative value for PFOS concentrations above  $\sim 4 \times 10^{-7} \text{ mol}\cdot\text{L}^{-1}$ . This also suggested that existence of an optimum concentration range for PFOS-induced fluorescence enhancement of NCDs, which was used for the PFOS detection.

## Conclusions

NCDs prepared through a hydrothermal method via vitamin B<sub>1</sub> as precursor and triethylamine as doping agent have been developed. The NCDs demonstrated strong photoluminescence emission with quantum yield of 12%, robust resistance against photobleaching, solution pH values, temperature, and ion strength. As fluorescent nanoprobe, it can be applied for the quantitative detection of PFOS with a high linear range and a low detection limit by virtue of the statically enhancement of fluorescence of NCDs. Satisfactory results were obtained for determination of PFOS in spiked real water samples.

**Acknowledgements** This work was supported by the National Natural Science Foundation of China (No. 21665018 and 21366024), Natural Science Foundation of Jiangxi Province (No. 20181BAB203014) and Foundation of Jiangxi Educational Committee (No. GJJ160724). This work was also supported by the "Graduate Student Innovation Funds for the Nanchang Hangkong University (No. YC2018-S361)".

**Compliance with ethical standards** The author(s) declare that they have no competing interests.

## References

- Giesy JP, Kannan K (2002) Perfluorochemical surfactants in the environment. *Environ Sci Technol* 36:146A–152A
- Carter KP, Young AM, Palmer AE (2014) Fluorescent sensors for measuring metal ions in living systems. *Chem Rev* 114:4564–4601
- Viberg H, Eriksson P (2011) Perfluorooctane Sulfonate and Perfluorooctanoic Acid[M], *Reproductive and Developmental Toxicology*, Elsevier
- Sanganyado E, Rajput IR, Liu W (2018) Bioaccumulation of organic pollutants in indo-Pacific humpback dolphin: a review on current knowledge and future prospects. *Environ Pollut* 237:111–125
- Yin N, Yang R, Liang S, Liang S, Hu B, Ruan T, Faiola F (2018) Evaluation of the early developmental neural toxicity of F-53B, as compared to PFOS, with an in vitro mouse stem cell differentiation model. *Chemosphere* 204:109–118
- Armitage JM, Schenker U, Scheringer M, Martin JW, MacLeod M, Cousins IT (2009) Modeling the global fate and transport of perfluorooctane sulfonate (PFOS) and precursor compounds in relation to temporal trends in wildlife exposure. *Environ Sci Technol* 43:9274–9280
- Daughton CG (2005) "Emerging" chemicals as pollutants in the environment: a 21st century perspective. *Renew Resour J* 23:6–23
- Thanh W, Yawei W, Chunyang L, Yaqi C, Guibin J (2009) Perspectives on the inclusion of perfluorooctane sulfonate into the Stockholm convention on persistent organic pollutants. *Environ Sci Technol* 43:5171–5175
- Environmental Protection Agency (EPA), Provisional Health Advisories for Perfluorooctanoic acid (PFOA) and Perfluorooctane Sulfonate (PFOS). [http://water.epa.gov/action/advisories/drinking/upload/2009\\_01\\_15\\_criteria\\_drinking\\_pha\\_PFOA\\_PFOS.PDF](http://water.epa.gov/action/advisories/drinking/upload/2009_01_15_criteria_drinking_pha_PFOA_PFOS.PDF). (Accessed July 2014)
- European Commission, Directive 2013/39/EU of the European Parliament and of the council of 12 august 2013 amending directives 2000/60/EC and 2008/105/EC as regards priority Substances in the field of water policy. *Official Journal of the European Union*, 2013, L226/1
- Sun RWM, Tang L, Li J, Qian Z, Han T, Xu G (2018) Perfluorinated compounds in surface waters of Shanghai, China: source analysis and risk assessment. *Ecotox Environ Safe* 149:88–95
- Zareitalabad P, Siemens J, Hamer M, Amelung W (2013) Amelung, Perfluorooctanoic acid (PFOA) and perfluorooctanesulfonic acid (PFOS) in surface waters, sediments, soils and wastewater—a review on concentrations and distribution coefficients. *Chemosphere* 91: 725–732
- Zacs D, Bartkevics V (2016) Trace determination of perfluorooctane sulfonate and perfluorooctanoic acid in environmental samples (surface water, wastewater, biota, sediments, and sewage sludge) using liquid chromatography-orbitrap mass spectrometry. *J Chromatogr A* 1473:109–121
- Munoz G, Labadie P, Geneste E, Pardon P, Tartu S, Chastel O, Budzinski H (2017) Biomonitoring of fluoroalkylated substances in Antarctica seabird plasma: development and validation of a fast and rugged method using on-line concentration liquid chromatography tandem mass spectrometry. *J Chromatogr A* 1513:107–117
- Lin M, Yang Y, Liu Y, Sun MX (2013) Trace analysis of perfluorooctane sulfonic acid in textile fabrics by gas chromatography/mass spectrometry with on-column derivatization. *Chinese J Anal Chem* 41:888–892



16. Sun YP, Zhou B, Lin Y, Wang W, Fernando KAS, Pathak P, Meziani MJ, Harruff BA, Wang X, Wang H, Luo PG, Yang H, Kose ME, Chen B, Veca LM, Xie SY (2006) Quantum-sized carbon dots for bright and colorful photoluminescence. *J Am Chem Soc* 128:7756–7757
17. Li H, Kang Z, Liu Y, Lee S-T (2012) Carbon nanodots: synthesis, properties and applications. *J Mater Chem* 22:24230–24253
18. Bandi R, Devulapalli NP, Dadigala R, Gangapuram BR, Guttena V (2018) Facile conversion of toxic cigarette butts to N,S-Codoped carbon dots and their application in fluorescent film, security ink, bioimaging, sensing and logic gate operation. *ACS Omega* 3: 13454–13466
19. Ding H, Du F, Liu P, Chen Z, Shen J (2015) DNA-carbon dots function as fluorescent vehicles for drug delivery. *ACS Appl Mater Inter* 7:6889–6897
20. Wang L, Li M, Li W, Han Y, Liu Y, Li Z, Zhang B, Pan D (2018) Rationally designed efficient dual-mode colorimetric/fluorescence sensor based on carbon dots for detection of pH and Cu<sup>2+</sup> ions. *ACS Sustain Chem Eng* 6:12668–12674
21. Moon BJ, Oh Y, Shin DH, Kim SJ, Lee SH, Kim TW, Park M, Bae S (2016) Facile and purification-free synthesis of nitrogenated amphiphilic graphitic carbon dots. *Chem Mater* 28:1481–1488
22. Yang S, Li Y, Wang S, Wang M, Chu M, Xia B (2018) Advances in the use of carbonaceous materials for the electrochemical determination of persistent organic pollutants. A review. *Microchim Acta* 185:112–125
23. Xiang GQ, Ren Y, Xia Y, Mao W, Fan C, Guo SY, Wang PP, Yang DH, He L, Jiang X (2017) Carbon-dot-based dual-emission silica nanoparticles as a ratiometric fluorescent probe for bisphenol a. *Spectrochim Acta A* 177:153–157
24. Liu G, Chen Z, Jiang X, Feng DQ, Zhao J, Fan D, Wang W (2016) In-situ hydrothermal synthesis of molecularly imprinted polymers coated carbon dots for fluorescent detection of bisphenol a. *Sensor Actuat B-Chem* 228:302–307
25. Wang Y, Ni P, Jiang S, Lu W, Li Z, Liu H, Lin J, Sun Y, Li Z (2018) Highly sensitive fluorometric determination of oxytetracycline based on carbon dots and Fe<sub>3</sub>O<sub>4</sub> MNPs. *Sensor Actuat B-Chem* 254:1118–1124
26. Cheng Z, Dong H, Liang J, Zhang F, Chen X, Du L, Tan K (2019) Highly selective fluorescent visual detection of perfluorooctane sulfonate via blue fluorescent carbon dots and berberine chloride hydrate. *Spectrochim Acta A* 207:262–269
27. Chen Q, Zhu P, Xiong J, Gao L, Tan K (2019) A sensitive and selective triple-channel optical assay based on red-emissive carbon dots for the determination of PFOS. *Microchem J* 145:388–396
28. Jiao Z, Li J, Mo L, Liang J, Fan H (2018) A molecularly imprinted chitosan doped with carbon quantum dots for fluorometric determination of perfluorooctane sulfonate. *Microchim Acta* 185:473–481
29. Shi L, Yang JH, Zeng HB, Chen YM, Yang SC, Wu C, Zeng H, Yoshihito O, Zhang Q (2016) Carbon dots with high fluorescence quantum yield: the fluorescence originates from organic fluorophores. *Nanoscale* 8:14374–14378
30. Jana J, Ganguly M, Chandrakumar KR, Mohan RG, Pal T (2016) Boron precursor dependent evolution of differently emitting carbon dots. *Langmuir* 33:573–584
31. Wu M, Wang Y, Wu W, Hu C, Wang X, Zheng J, Li Z, Jiang B, Qiu J (2014) Preparation of functionalized water-soluble photoluminescent carbon quantum dots from petroleum coke. *Carbon* 78:480–489
32. Reckmeier CJ, Wang Y, Zboril R, Rogach AL (2016) Influence of doping and temperature on solvatochromic shifts in optical spectra of carbon dots. *J Phys Chem C* 120:10591–10604
33. Haijuan Z, Yonglei C, Meijuan L, Laifang X, Shengda Q, Hongli C, Xingguo C (2014) Solid-phase synthesis of highly fluorescent nitrogen-doped carbon dots for sensitive and selective probing ferric ions in living cells. *Anal Chem* 86:9846–9852
34. Wu F, Zhu J, Tan K (2012) Resonance light scattering spectra of perfluorooctane sulfonate-protein system and its analytical application. *Chinese J Appl Chem* 29:969–973
35. Zuo P, Lu X, Sun Z, Guo Y, Hua H (2016) A review on syntheses, properties, characterization and bioanalytical applications of fluorescent carbon dots. *Microchim Acta* 183:519–542

**Publisher's note** Springer Nature remains neutral with regard to jurisdictional claims in published maps and institutional affiliations.